

ARM Cloud Parameterization and Modeling Working Group – GCSS Polar Cloud Working Group Model Intercomparison

Procedures for ARM CPMWG Case 5 /

*GCSS Polar Cloud WG SCM/CRM/LES Intercomparison Case f2004:
ARM Mixed-Phase Arctic Cloud Experiment (M-PACE): October 5-22, 2004*

Stephen Klein¹, Ann Fridlind², Renata McCoy¹, Greg McFarquhar³, Surabi Menon⁴, Hugh Morrison⁵, Dana Veron⁶, Shaocheng Xie¹, J. John Yio¹, Minghua Zhang⁷

1. LLNL
2. NASA/GISS
3. U. Illinois
4. LBNL
5. NCAR/UCAR
6. U. Delaware
7. SUNY Stony Brook

*This document is available from the ARM CPMWG SCM Case 5 Intercomparison Web page:
<http://science.arm.gov/wg/cpm/scm/scmic5>*

Contents

1 Introduction

1.1 Strategy

1.2 Case Description

Period B

Period A

1.3 Aircraft Data

2 Protocol

2.1 Period B specifications

Initial and lower boundary conditions

Large-scale forcing

Aerosol specifications

2.2 Period A specifications

Initial and lower boundary conditions

Large-scale forcing

Aerosol specifications

3 Sensitivity studies

4 Results to Submit

4.1. Description of Experimental Quantities

4.1.1 Vertical profile quantities

4.1.2 Time-series quantities

- 4.1.3 How these quantities are to be directed to files, and how the files named
- 4.2. Formats for Data Files to be Submitted
 - 4.2.1 Format for a .p file containing a profile variable
 - 4.2.2 Format for time series quantities for a .t file, containing time-series variables

5 Model Descriptions

6 Time Table

- 6.1 Soliciting & Accepting Preliminary Results
- 6.2 Processing & Comparing Preliminary Results
- 6.3 Results Discussion

1 Introduction

1.1 Strategy

This intercomparison is formulated to address the parameterization of clouds in climate models by using ARM (Atmospheric Radiation Measurement) data and by building on the ARM/ the Global Energy and Water Cycle Experiment (GEWEX) Cloud System Study (GCSS) intercomparison experiences from previous cases.

In particular, the science theme of this intercomparison is: what determines the microphysical properties of mixed phase Arctic clouds in observations and models? Comparison to available ARM aircraft and other data is employed to evaluate model microphysical simulations. The goals of this intercomparison are to (a) document the current state of mixed-phase cloud microphysics in models as they perform under two types of complex mixed-phase conditions that commonly occur in the Arctic, (b) understand the sources of differences between models in their simulations of mixed phase cloud microphysics, and (c) use the data provided by the M-PACE to spur improvements in the representation of mixed phase cloud microphysics in climate and cloud resolving models.

This intercomparison is based on the 17.5-day ARM program Intensive Observing Period (IOP) that took place over the North Slope of Alaska (NSA) in October 2004. During this IOP, a sounding network of four stations was in place which launched 6-hourly radiosondes for most of the experiment. From these soundings and other data such as analyses from the European Centre for Medium Range Weather Forecasts (ECMWF), the LLNL ARM team has derived the large-scale advective forcings that can be used to drive Single Column and Cloud Resolving Models (SCMs and CRMs). The variational analysis was derived by applying the method of Zhang and Lin (1997)¹ and Zhang et al. (2001)² to the available data. Further details about the advective

¹ Zhang, M. H., and J. L. Lin (1997), *Constrained variational analysis of sounding data bases on column-integrated budgets of mass, heat, moisture, and momentum: Approach and application to ARM measurements*. *J. Atmos. Sci.*, **54**, 1503-1524.

² Zhang, M. H., J. L. Lin, R. T. Cederwall, J. J. Yio, and S. C. Xie (2001), *Objective analysis of ARM IOP Data: Method and sensitivity*. *Mon. Weather Rev.*, **129**, 295-311.

forcing (see Xie et al. 2005)³ are available from the intercomparison web page listed above. (Note that this analysis is to be used for only one of the two periods, as described below).

1.2 Case Description

For this intercomparison, we will focus on two periods. Figure 1 shows the time-height distribution of clouds from the ARM cloud radar and other sensors at Barrow as derived with the ARSCL (Active Remote Sensing of Clouds) algorithm (Clothiaux et al. 2000)⁴.

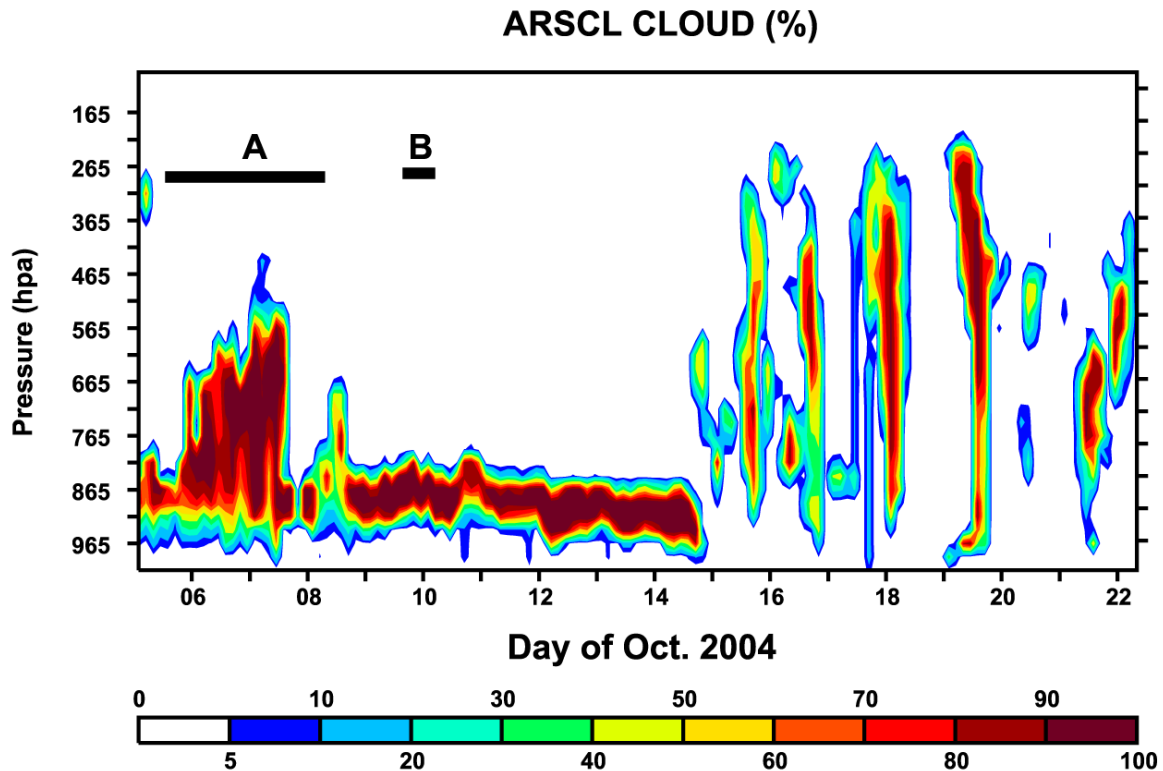


Figure 1. ARSCL Cloud Frequency during October 2004.

This intercomparison will contrast the microphysics of multi-layer stratus present on 5-8 October (Period A) with those of the single layer stratocumulus present in the period 9-14 October (Period B). During both periods mixed phase clouds were present with cloud temperatures varying between -5 and -20C. These two periods were selected because of the differing nature of the cloud systems. Some description and observations from these periods are now given. We begin with Period B as this is a simpler case and one that is better observed and described.

³ Xie, S., S. A. Klein, M. Zhang, J. J. Yio, R. T. Cederwall, and R. McCoy, 2006: *Developing large-scale forcing data for single-column model and cloud-resolving model from the Mixed-Phase Arctic Cloud Experiment*. *J. Geophys. Res.*, submitted.

⁴ Clothiaux, Eugene E, Thomas P Ackerman, Gerald G Mace, Kenneth P Moran, Roger T Marchand, Mark Miller, and Brooks E Martner. 2000. Objective determination of cloud heights and radar reflectivities using a combination of active remote sensors at the ARM CART Sites. *Journal of Applied Meteorology*, 39, 645-665.

Period B

During Period B, single layer boundary layer mixed-phase clouds formed as a result of east-northeast flow which brought cold near-surface air from the sea-ice located about 500 km to the north over the warm open ocean that was adjacent to the Alaska north coast. Under these “cold-air outbreak” conditions, there were large ocean sensible and latent heat fluxes which combined with the conditions of general subsidence promoted a well-mixed cloudy boundary layer. These clouds then advected to the Alaskan coast where they were observed at Barrow and Oliktok Point. The composite visible satellite image from the NASA Terra satellite for October 9, 2004 displays the characteristic cold-air outbreak cloud structure in which rolls of small horizontal size broaden in scale as the air flows downstream (Figure 2).

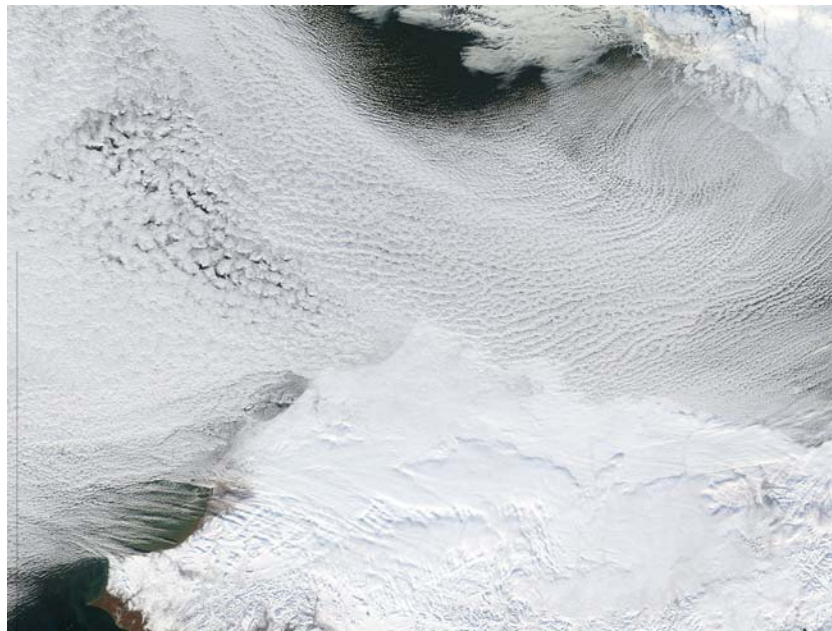


Figure 2. Composite visible satellite image from the NASA Terra satellite for October 9, 2004.

The microphysical properties of this cloud system were sampled by two Citation flights during Period B (The aircraft data which are central to this intercomparison will be described more fully in the following section). Figure 3 shows the liquid water content and temperature from one spiral; the data shows that the liquid water content increases with height above cloud base as would be expected for a stratocumulus cloud at the top of a well-mixed boundary layer. Figure 4 shows a significant amount of ice was also present both in the cloud and beneath the liquid water cloud base. In general, liquid dominated near the tops of the clouds with precipitating ice (sometimes heavy) near the base – although it is noted that considerable variability exists between spirals. The microwave radiometer liquid water path during Period B averaged 225 g m^{-2} at Barrow and 285 g m^{-2} at Oliktok Point.

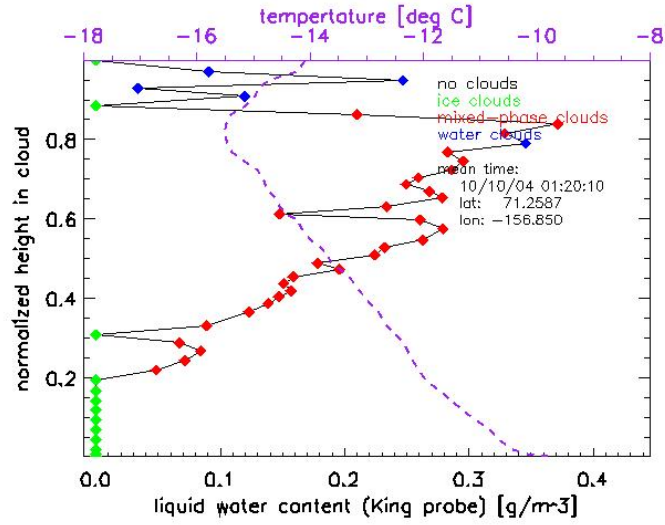


Figure 3. Liquid water content and temperature from a Citation spiral during Period B. The vertical axis is altitude normalized by the top and bottom of cloud. For example, a normalized height of 0.5 is in the middle of the cloud.

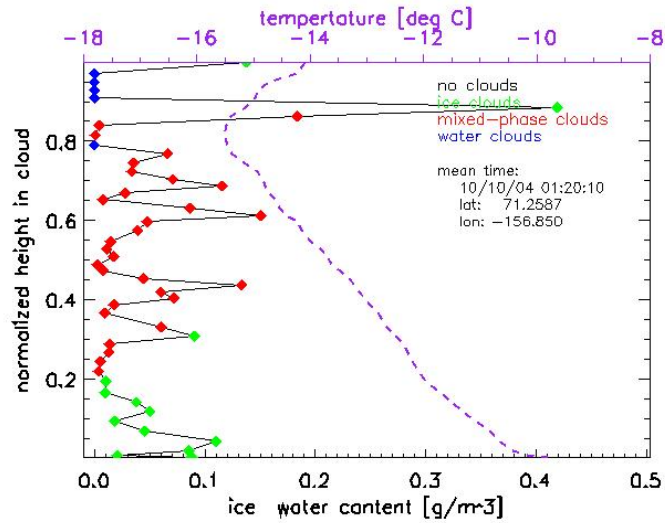


Figure 4. As in Figure 3, but for ice water content.

Period A

The conditions of Period A are considerably different. In this period, a low level disturbance entered the North Slope of Alaska region from the east. As analyzed below, there was upward vertical velocity beneath 500 hPa and subsidence above promoting the formation of the clouds in the lower troposphere. Figures 5 and 6 show the liquid and ice water contents and temperature for a spiral during the October 6th flight. Several liquid water layers are present; these layers tend to occur at the base of small inversions and in relatively unstable layers suggesting a significant amount of turbulent mixing was occurring. In contrast, ice water content was present throughout the vertical extent of the cloud suggesting that ice crystals were settling between the different liquid water layers.

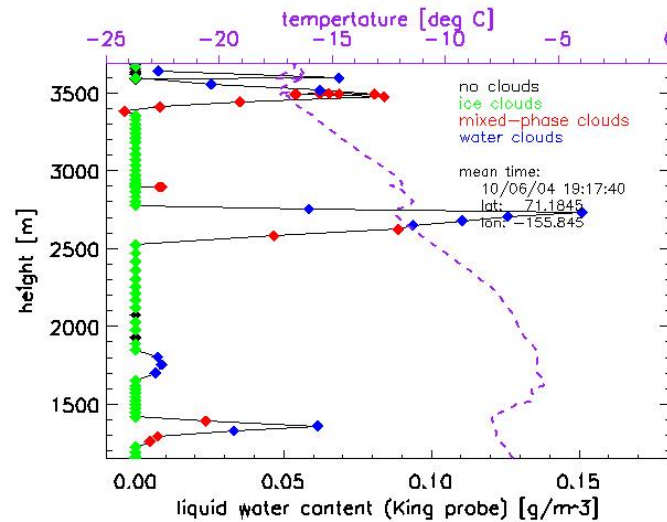


Figure 5. Liquid water and temperature from a Citation spiral during Period A.

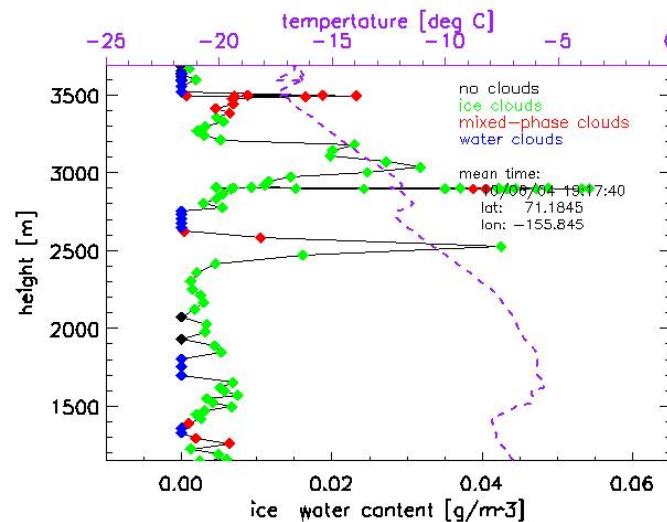


Figure 6. As in Figure 5 but for ice water content.

A striking display of this multi-layer cloud structure was captured by the Arctic High Spectral Resolution Lidar (Figure 7). The lower panel of this figure shows the depolarization ratio for the last 12 hours of October 6. In general, regions of low depolarization ratio indicate liquid water dominant layers and regions of high depolarization ratio indicate ice dominant layers. Similar to the aircraft data, the lidar suggests that there were several thin liquid water layers with ice crystals settling between the layers. For example, near 21Z three liquid water layers are present near 1, 2 and 3 kilometers. The liquid water path from the microwave radiometers is considerably lower during Period A than it was during Period B, averaging about 50 g m^{-2} from the data taken at Barrow, Atkasuk, and Oliktok Point.

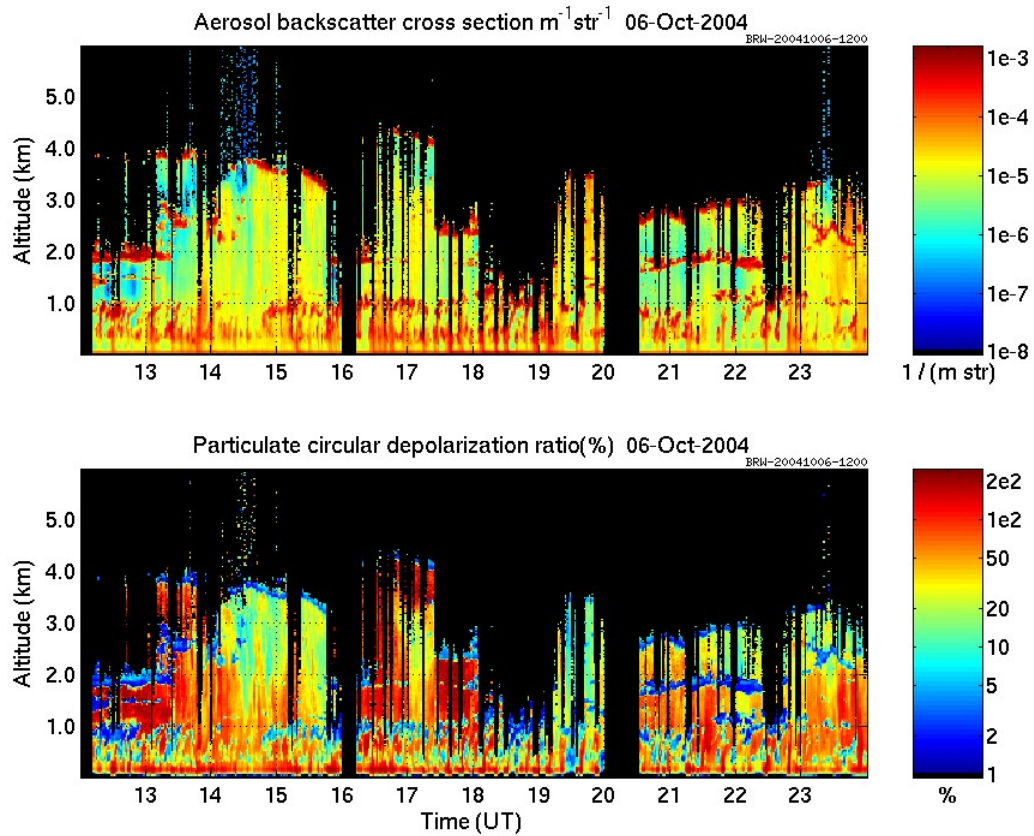


Figure 7. Aerosol backscatter cross section and depolarization ratio from the Arctic High-Spectral Resolution Lidar for 12Z October 6 to 00Z October 7, 2004 at Barrow.

1.3 Aircraft Data

Central to this intercomparison are the evaluation data provided by the microphysical instruments on the University of North Dakota (UND) Citation aircraft. During Period A there were 2 UND Citation flights on October 5th and 6th (none on the 7th) and during Period B there were two flights on October 9th. The flights on October 10th and 12th are also of interest because they occurred in clouds similar in structure to those observed on October 9th.

The Citation was equipped with a range of probes for measuring the sizes, shapes and phases of the complete range of hydrometeors that can be sampled within a cloud. In particular, it had a two-dimensional cloud (2DC) probe effectively measuring size distributions (SDs) between 125 and 1600 μm , a one dimensional cloud (1DC) probe that measures particles with diameters between 50 and 620 μm , a forward scattering spectrometer probe (FSSP) that measures particles with diameters between 3.0 and 54.5 μm and a high-volume precipitation sampler (HVPS) that measures particles with diameters between 400 μm to 4 cm. A CPI (Cloud Particle Imager) provided 2.3 μm resolution images for particles with diameters between 15 and 2000 μm . Bulk water content was measured with a King LWC probe and a CSI (Cloud Spectrometer and Impactor) probe (a newer version of the CVI– Counterflow Virtual Impactor) gave bulk measurements of TWC. A Rosemount icing detector identified the presence of supercooled water. This combination of probes gives the information needed to determine the phase, size distributions and bulk cloud microphysical properties covering the entire size range of hydrometeors in mixed-phase clouds. The phase identification algorithm and calculation of bulk microphysical properties from these data follow the techniques used by McFarquhar and Cober (2004)⁵ to calculate the same quantities from SHEBA and FIRE ACE data. Bulk microphysical properties that can be derived from these data for comparison to models include the liquid water content (LWC), ice water content (IWC), liquid water fraction (LWC/TWC), effective radius of cloud droplets ($r_{\text{eff},l}$), effective radius of ice crystals ($r_{\text{eff},i}$), total liquid cloud droplet number concentration and total ice crystal number concentration. Because there exist multiple definitions of $r_{\text{eff},i}$ (McFarquhar and Heymsfield 1998)⁶, the definition of Fu (1996)⁷ is used here because it preserves the ratio between the ice mass content IWC and cross-sectional area A_c of the particle distributions, and hence is most appropriate for determining the radiative effects of clouds. $r_{\text{eff},i}$ is given by

$$r_{\text{eff},i} = \frac{\sqrt{3}IWC}{3\rho_i A_c}$$

where ρ_i is the bulk density (mass divided by volume) of the ice crystals.

⁵ McFarquhar, G. M., and S. G. Cober, 2004: Single-scattering properties of mixed-phase Arctic clouds at solar wavelengths: impacts on radiative transfer. *J. Climate*, 17, 3799–3813.

⁶ McFarquhar, G. M., and A. J. Heymsfield, 1998: The definition and significance of an effective radius for ice clouds. *J. Atmos. Sci.*, 55, 2039–2052

⁷ Fu, Q., 1996: An accurate parameterization of the solar radiative properties of cirrus clouds. *J. Climate.*, 9, 2058–2082

Figure 8 shows an example of size distributions measured as a function of height on October 10. At the time of this spiral, the lidar at Oliktok Point detected cloud base at 900 m and a strong liquid layer near cloud top at 1300 m under a sharp inversion. Liquid layers are seen by strong peaks in the FSSP size distribution around 20 μm , with the modal diameter increasing with height due to condensational growth. In general, greater numbers of large crystals, corresponding to ice, are seen near cloud base (1000 and 1100 m) and precipitating beneath (700 and 800 m), but ice occurs in patches throughout the cloud.

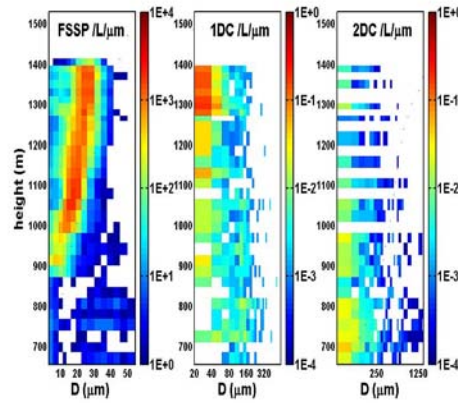


Figure 8. Vertical profile of 10-s averaged size distributions as measured by FSSP, 1DC, 2DC for spiral flow over Oliktok Point, October 10, 2004.

Figure 9, produced from all of the spirals flown on October 10 in single-layer mixed phase clouds shows how the fraction of ice mass in the cloud, $1-f_l$, where $f_l = \text{LWC}/(\text{LWC}+\text{IWC})$, varies with the normalized cloud altitude z_n (where $z_n = 0$ at cloud base and $z_n = 1$ at cloud top). Figure 9 shows that the ice fraction of cloud mass is larger near cloud base where the larger more massive ice crystals have settled to, and is not a simple function of temperature.

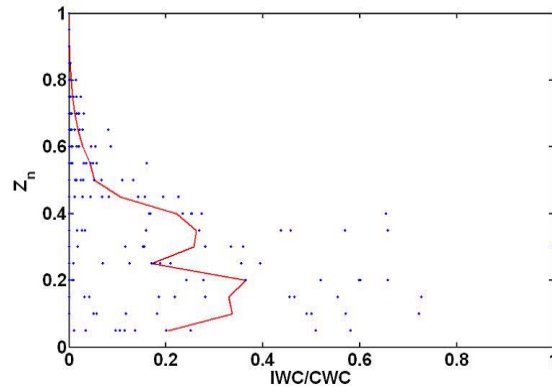


Figure 9. Vertical variation of fraction of ice IWC/CWC ($1-f_l$) in terms of z_n .

Figure 10 shows the vertical distribution of the effective radius of cloud droplets ($r_{eff,l}$) and ice crystals ($r_{eff,i}$). $r_{eff,l}$ increases with height above cloud base, as is typical for well-mixed stratocumulus, whereas $r_{eff,i}$ is relatively constant. Similar types of plots can be derived for all mixed-phase cloud bulk properties from all spirals for comparison to models.

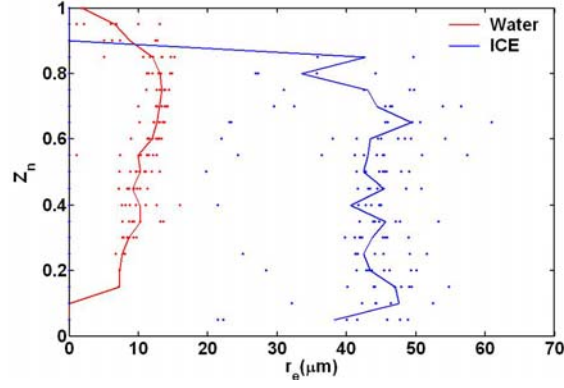


Figure 10. As in Fig. 9 except for variation of $r_{eff,l}$ and $r_{eff,i}$.

2 Protocol

In this section, the prescription for the initial condition and forcing data for all models is given. Note that these prescriptions differ according to the period!

2.1 Period B specifications

The period of simulation is from 17Z October 9 to 5Z October 10. This period is only 12 hours long so that Large-eddy simulation models may participate in this intercomparison.

Initial and lower boundary conditions

1. Use the file `initial.sounding.dry.ascii` which is available from the CPM web page <http://science.arm.gov/wg/cpm/scm/scmic5/docs/initial.sounding.dry.ascii>.
2. The specifications that created this initial sounding are given below.
 - Lower boundary condition is an ocean with temperature 274.01K (or 0.85C)
 - Latitude/Longitude is 71.75N, 151W
 - Surface pressure $p_s = 1010$ mb
 - Inversion pressure $p_{inv} = 850$ mb
 - Liquid water potential temperature $\theta_l(p > p_{inv}) = 269.2$ K
 - Total water mixing ratio $q_t(p > p_{inv}) = 1.95$ g/kg
 - Potential temperature $\theta(p < p_{inv}) = 275.33\text{K} + 0.0791 \text{ K/mb} * (815 \text{ mb} - p)$
 - Water vapor mixing ratio $q(p < p_{inv}) = 0.291 \text{ g/kg} + 0.00204 \text{ g/kg/mb} * (p - 590 \text{ mb})$
With this specification, the water vapor mixing ratio immediately above the inversion is 0.8214 g/kg.
3. The model must be initialized with an adiabatic profile of liquid water - this profile is provided in the initial sounding file. Note that there is no ice present at the initial time. We expect that the models will produce ice after the initial time and that a microphysical steady state will be achieved within a few hours after the start of the simulation.
4. Winds are constant with height with the zonal wind of -13 m/s and meridional wind of -3 m/s. The profile of winds is provided in the initial sounding file.

These initial conditions are displayed in Figures 11 and 12.

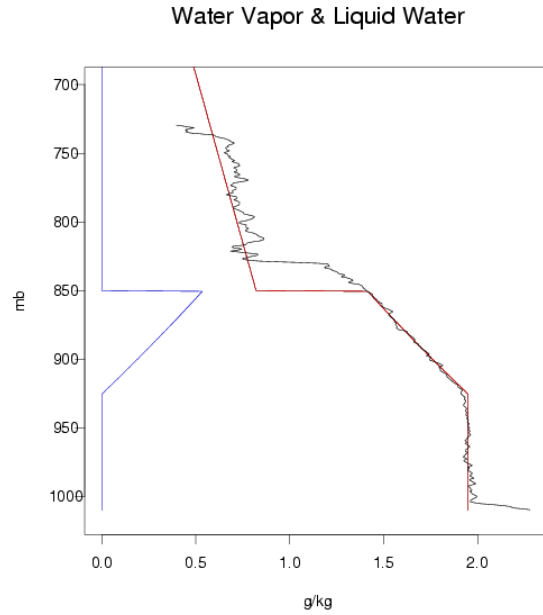


Figure 11. Initial condition of water vapor (red line) and liquid water (blue line) mixing ratio for Period B. Also shown is the 17Z October 9 sounding from Barrow (black line).

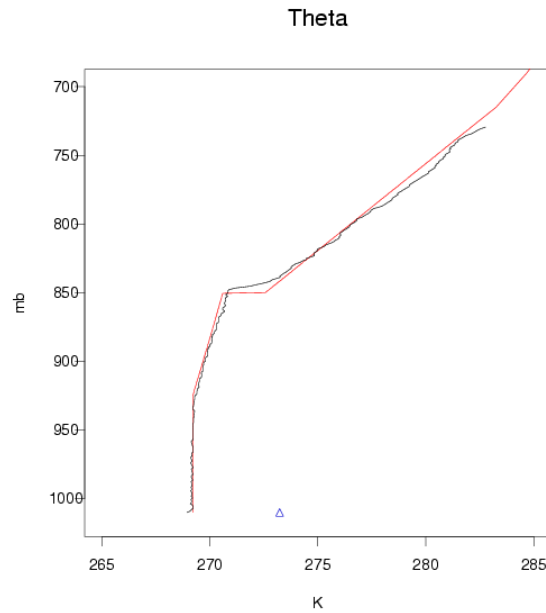


Figure 12. Initial condition of potential temperature (red line) for the models. The black line shows the potential temperature from the 17Z October 9 sounding. The triangle indicates the value of the ocean temperature potential temperature (i.e. the potential temperature corresponding to the ocean absolute temperature at the observed surface pressure of 1010 hPa).

Large-scale forcing

The large-scale forcing for all models is to be held constant for the duration of the 12 hour simulation. These forcings (Figure 13) were derived from an analysis of the ECMWF model data for the ocean region adjacent to the North Slope of Alaska (Figure 14).

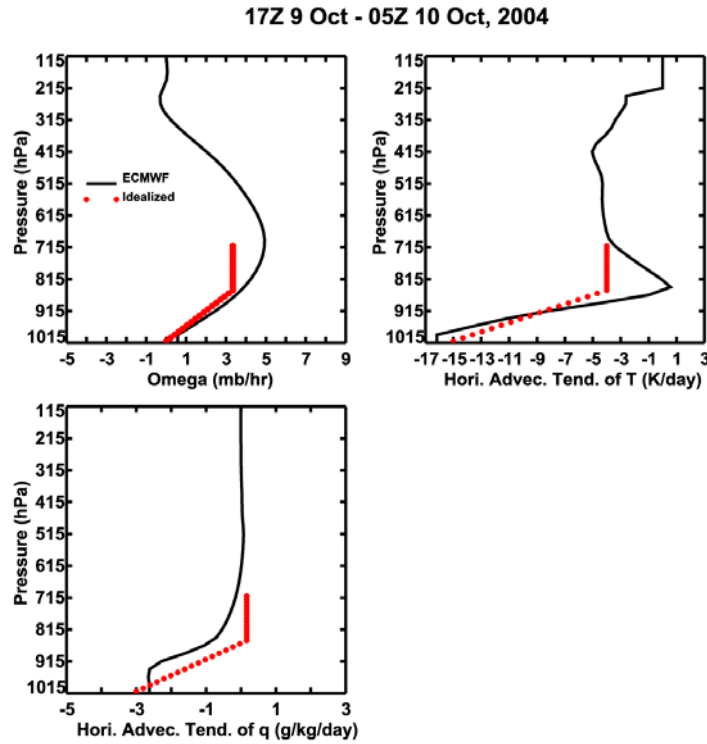


Figure 13. Vertical pressure velocity omega and the horizontal advective tendencies of temperature and water vapor from the ECMWF analyses (black line) and their idealizations (red dots) which are to be used in model simulations of Period B.

Analysis Domain For ECMWF Data

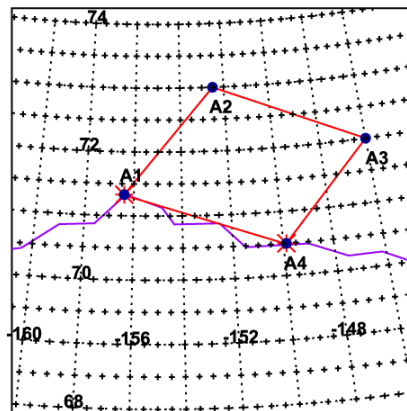


Figure 14. The analysis domain over which the ECMWF model data is averaged.

Details of the forcings are:

1. The vertical pressure velocity omega is

$$\min [D^*(p_s-p) , D^*(p_s-p_{inv})]$$

where “min” is the minimum operator and D is the horizontal wind divergence. In Period B, D is $5.8 \times 10^{-6} \text{ s}^{-1}$.

2. The temperature tendency from horizontal advection is

$$\min [-4, -15*(1 - ((p_s-p)/218.18 \text{ mb}))] \text{ K/day (note that } p \text{ and } p_s \text{ are in mb)}$$

3. The water vapor mixing ratio tendency from horizontal advection is

$$\min [0.164, -3*(1 - ((p_s-p)/151.71 \text{ mb}))] \text{ g/kg/day}$$

4. The potential temperature θ tendency from vertical advection is

$$- \text{omega} * d\theta/dp$$

where omega is specified from number 1 above but $d\theta/dp$ is calculated from the model. Note that the physical temperature T tendency from vertical advection is

$$- (T/\theta) * \text{omega} * d\theta/dp$$

where (T/θ) is calculated using the mean physical and potential temperatures of a given level.

5. The water vapor mixing ratio tendency from vertical advection is

$$- \text{omega} * dq/dp$$

where omega is specified from number 1 above but dq/dp is calculated from the model.

6. The tendency of other tracers X (e.g. cloud variables) due to vertical advection is

$$- \text{omega} * dX/dp .$$

7. The horizontal advection tendency of all tracers save water vapor and temperature is unknown and is set to zero.

8. The description and explanation for the forcing above is the following:

The subsidence velocity linearly increases from the surface until the inversion where it is fixed at $\sim 80 \text{ mb/day}$ for all altitudes above that point. The horizontal advective tendencies of temperature

and water vapor mixing ratio are linear with pressure beneath the inversion and held at a constant value above the inversion.

For moisture above the inversion, there should be no drift with time. This is because the moistening rate above the inversion due to horizontal advection of 0.164 g/kg/day is chosen so that it exactly cancels the tendency of water vapor mixing ratio due to vertical advection.

For temperature above the boundary layer, the cooling rate due to horizontal advection is specified as 4 K/day cooling. If the radiative cooling rate is ~ 2 K/day (not unreasonable), this will approximately balance the subsidence warming rate which from point number 4 above is ~ 6 K/day.

9. Above 700 hPa, all variables should be fixed at their initial values.

10. Surface fluxes are to be specified at the ECMWF values of 136.5 W m⁻² sensible and 107.7 W m⁻² latent heat. Thus the primary role of the ocean temperature is in radiation calculations to calculate, for example, the upward longwave radiation at the surface.

11. Winds should be kept close to their initial values. We recommend nudging with a time scale of 1 or 2 hours, but models are free to choose their prescriptions.

12. Radiation should be interactive and calculated with whatever means are available. Radiation codes may require an vertical profile ozone. An ozone profile is available from the arctic profile available from SCM intercomparison web site under forcing data. For radiation purposes, the lower boundary is an open-ocean surface with low albedo. LES models may require the amount of longwave radiation at the top of their domain. A prescription for this will be forthcoming.

Aerosol specifications

As the interaction between clouds and aerosols may be crucial to the microphysical structure of mixed-phase clouds, the following information is provided for those models whose microphysics depends on the characterization of aerosols.

The aerosol size distribution has been obtained from a Hand-Held Particle Counter (HHPC-6) on board the Aerosonde unmanned aerial vehicle (UAV), and a condensation nuclei (CN) counter from the NOAA Climate Monitoring Diagnostics Laboratory (CMDL) located near Barrow (but away from local pollution sources). A bimodal dry lognormal aerosol size distribution has been fitted to the average size-segregated HHPC-6 measurements from 10/10/04, with the total aerosol concentration constrained by the average CMDL CN measurements. The HHPC-6 observations and fitted curve are shown in Figure 15. The size distribution for each mode of the lognormal distribution is given by

$$\frac{dN}{d \ln r} = \frac{N_t}{\sqrt{2\pi} \ln \sigma} \exp \left[-\frac{\ln^2(r/r_m)}{2 \ln^2 \sigma} \right]$$

The fitted aerosol parameters σ , r_m , and N_t are the standard deviation, geometric mean, and total number concentration of each mode, respectively. For mode 1 (smaller), these values are 2.04, 0.052 μm , and 72.2 cm^{-3} , respectively. For mode 2 (larger), these values are 2.5, 1.3 μm , and 1.8 cm^{-3} , respectively.

For aerosol composition, we recommend assuming ammonium bisulfate if a uniform composition is assumed for activation of accumulation-mode particles, based on field evidence for likely lack of full neutralization under remote Arctic conditions after transport over ocean (e.g., Fridlind et al., 2000⁸). However, we also recommend assuming an insoluble fraction of order 30% based on field evidence for deviations of activation behavior from uniform composition (Bigg and Leck, 2001⁹; Zhou et al., 2001¹⁰).

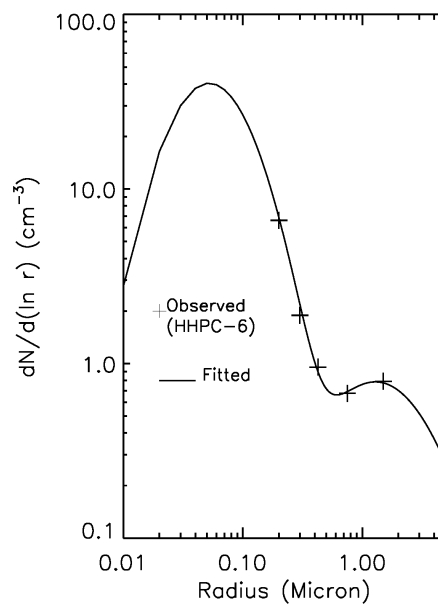


Figure 15. Observed and fitted dry aerosol size distribution.

The number concentration of active ice nuclei is obtained from in-situ out-of-cloud measurements on October 9 and 10 from the Continuous Flow Diffusion Chamber (CFDC) (Rogers et al., 2001¹¹) aboard the Citation aircraft (data provided by A. Prenni and P. DeMott). These measurements represent the sum of ice nuclei with a diameter less than 2 μm acting in deposition, condensation-freezing, and immersion-freezing modes. They indicate locally high

⁸ Fridlind, A. M., M. Z. Jacobson, V.-M. Kerminen, R. E. Hillamo, V. Ricrad, and J.-L. Jaffrezo, 2000: Analysis of gas-aerosol partitioning in the Arctic: Composition of size-resolved equilibrium model results with field data, *J. Geophys. Res.*, 105, 19891-19904.

⁹ Bigg, E. K., and C. Leck, 2001: Cloud active particles over the central Arctic Ocean, *J. Geophys. Res.*, 106, 32155-32166.

¹⁰ Zhou, J., E. Swietlicki, O. H. Berg, P. P. Aalto, K. Hameri, E. D. Nilsson, and C. Leck, 2001: Hygroscopic properties of aerosol particles over the central Arctic Ocean during summer, *J. Geophys. Res.*, 106, 32111-32124.

¹¹ Rogers, D. C., P. J. DeMott, S. M. Kreidenweis, and Y. Chen, 2001: A continuous-flow diffusion chamber for airborne measurements of ice nuclei, *J. Atmos. Ocean. Technol.*, 18, 725-741.

concentrations of ice nuclei up to $\sim 10 \text{ L}^{-1}$, and a mean value of about 0.16 L^{-1} assuming that concentrations below the detection threshold are zero. Data are plotted as a function of processing temperature and ice supersaturation in Figure 16. No direct measurements are available for the number of ice nuclei acting in contact-freezing mode.

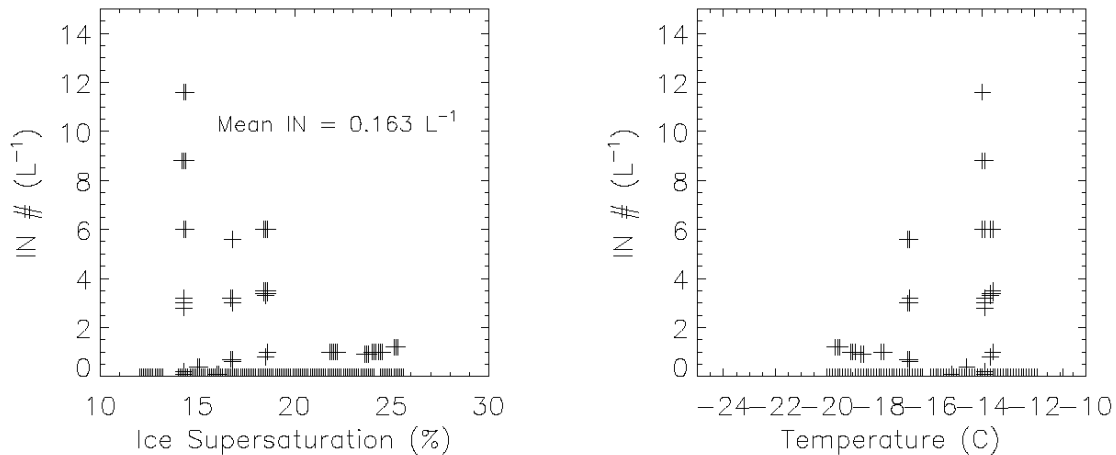


Figure 16. Out-of-cloud CFDC ice nuclei measurements from October 9 and 10 as a function of processing ice supersaturation and temperature.

2.2. Period A Specifications

The specifications for Period A will follow those that have been used in the many ARM CPM intercomparisons for the ARM Southern Great Plains site. If you have done this before little is changed except that (a) latitude/longitude is different, (b) surface albedo should be specified (as was done for the March 2000 case) because of snow on the ground. Note that the position for Period A is a land surface (in contrast to Period B where it is an ocean surface).

The period of simulation is from 14Z October 5 to 14Z October 8.

Initial and lower boundary conditions

For this period, both the initial conditions and large-scale forcings will be taken from the ARM variational analysis. This analysis is available from the ARM IOP Archive; information on how to acquire this analysis is on the CPM MPACE web page¹².

The initial profiles are based on the observed area averages of temperature, water vapor mixing ratio, and horizontal wind velocity for the M-PACE region. These are provided as functions of pressure at DP mb intervals from BOT to TOP mb. For the values derived by Zhang's variational analysis, $DP = 25$ mb, $BOT = 1015$ mb, and $TOP = 90$ mb. The values

¹² <http://science.arm.gov/wg/cpm/scm/scmic5>

provided must be interpolated to each model's vertical grid levels. Special treatment is necessary at the surface and the top of the variational analysis.

Regarding conditions to be specified at the ground, note that the lowest layer ($BOT = 1015$ mb) could be below the surface. Please use the provided domain-averaged surface pressure to set the surface boundary condition in your model. \bar{T} , \bar{q} , \bar{u} and \bar{v} at the surface can be obtained by extrapolation if the corresponding surface data are not available. $(\partial\bar{T}/\partial\alpha)_{L.S.}$, $(\partial\bar{q}/\partial\alpha)_{L.S.}$ and $\bar{\omega}$ are assumed to be zero at the surface. Values for model levels below BOT mb can be obtained by interpolation using values at BOT and the surface.

At the top of the model, the initial conditions should be handled differently from the tendencies. For the state variables \bar{T} and \bar{q} , use the values from the arctic profile on the web site at levels 215 hPa and above (Note this means replacing the analysis values of \bar{T} and \bar{q} between 90 hPa and 215 hPa with those from this arctic profile). The arctic profile is available from the SCM Intercomparison web page under forcing data. For \bar{u} and \bar{v} at levels above 90 hPa, use the values given at TOP mb. To obtain values of $\bar{\omega}$, $(\partial\bar{T}/\partial\alpha)_{L.S.}$ and $(\partial\bar{q}/\partial\alpha)_{L.S.}$ for model levels above TOP mb by interpolation, the simplest approach is to assume that $\bar{\omega}$, $(\partial\bar{T}/\partial\alpha)_{L.S.}$ and $(\partial\bar{q}/\partial\alpha)_{L.S.}$ are equal to zero at 20 km.

Models are asked to compute radiation using whatever means that they have available. Because radiative transfer calculations require temperature, water vapor mixing ratio, and ozone mixing ratio profiles above the top of the variational analysis, use the arctic profile available from the SCM Intercomparison web page.

We ask you to model the lower surface as land. The time-varying values of surface sensible and latent heat flux should be specified in your model from the analysis. Also radiation calculations will require the surface skin temperature and albedo. The time-varying skin temperature is provided in the analysis and the broadband visible albedo may be specified as 0.85 constant in time (i.e. the surface was snow covered). For diagnostic purposes, other surface quantities are provided at 3-hourly intervals. These include the surface pressure, the near-surface winds, the downwelling and upwelling solar and IR radiation, and precipitation. The average elevation of the M-PACE domain is 31.5 m.

Large-scale forcing

The primary large-scale forcing terms in the SCM/CRM governing equations are the large-scale advective tendencies of temperature, and water vapor mixing ratio. The large-scale forcings are based on observations averaged over the 4-sided variational analysis grid for M-PACE region which has an approximate rectangle-shape with dimension of about 240 km x 100 km and centered at 154W, 70.5N. The analysis domain is shown in Figure 17.

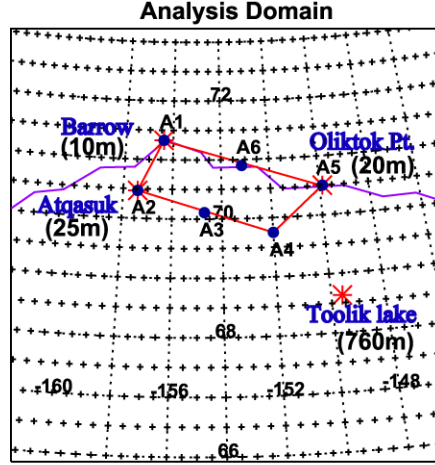


Figure 17. “●” symbols represent the analysis grids, “*” symbols are the locations of sounding stations, and “+” symbols denote the ECMWF model output grids

The advective forcing will be specified using the total (sometimes called “revealed”) advective forcing. The description of this forcing is below.

The large-scale advective tendencies for temperature \bar{T} and water vapor mixing ratio \bar{q} are formally defined (on isobaric surfaces) as

$$\left(\frac{\partial \bar{T}}{\partial t} \right)_{L.S.} \equiv -\bar{v} \cdot \nabla \bar{T} - \omega \frac{\partial \bar{T}}{\partial p} + \frac{\omega}{c_p} \alpha$$

and

$$\left(\frac{\partial \bar{q}}{\partial t} \right)_{L.S.} \equiv -\bar{v} \cdot \nabla \bar{q} - \omega \frac{\partial \bar{q}}{\partial p}$$

where ∇ is the horizontal del operator and α is the specific volume of air (the inverse of air density). Note that for potential temperature

$$\left(\frac{\partial \bar{\theta}}{\partial t} \right)_{L.S.} = \left(\frac{p_0}{\bar{p}} \right)^{R/c_p} \left(\frac{\partial \bar{T}}{\partial t} \right)_{L.S.}$$

The above terms can be calculated from the data provided in the analysis. Unfortunately, observations of the advective tendencies for hydrometeors are not available.

Profile values are given at 25-mb intervals for the ARM/SUNY variational analysis, and at 3-hour intervals. These values must be interpolated in pressure to the model's grid and in time.

Note: use *Horizontal_Temp_Advec* + *Vertical_s_Advec* for total advective temperature tendency to account for adiabatic compression term. Several temperature terms can be converted to potential temperature using the conversion:

$$\bar{\theta} = \left(\frac{p_0}{\bar{p}} \right)^{R/c_p} \bar{T}$$

where p_0 is 1000 mb.

For horizontal wind, we suggest that you nudge the model prognosed values with time scale of 1 or 2 hours to the time and height dependent values recorded in the analysis data.

Figure 18 shows the evolution of vertical velocity and the tendencies from horizontal advection of temperature and water vapor from the variational analysis during Period A. Also shown is the ARSCL cloud from Barrow. Note how the multilayer cloud formed in a condition of general uplift and that a strong moistening and cooling occurred near 20Z October 5 to aid in the formation of the multi-layer stratus.

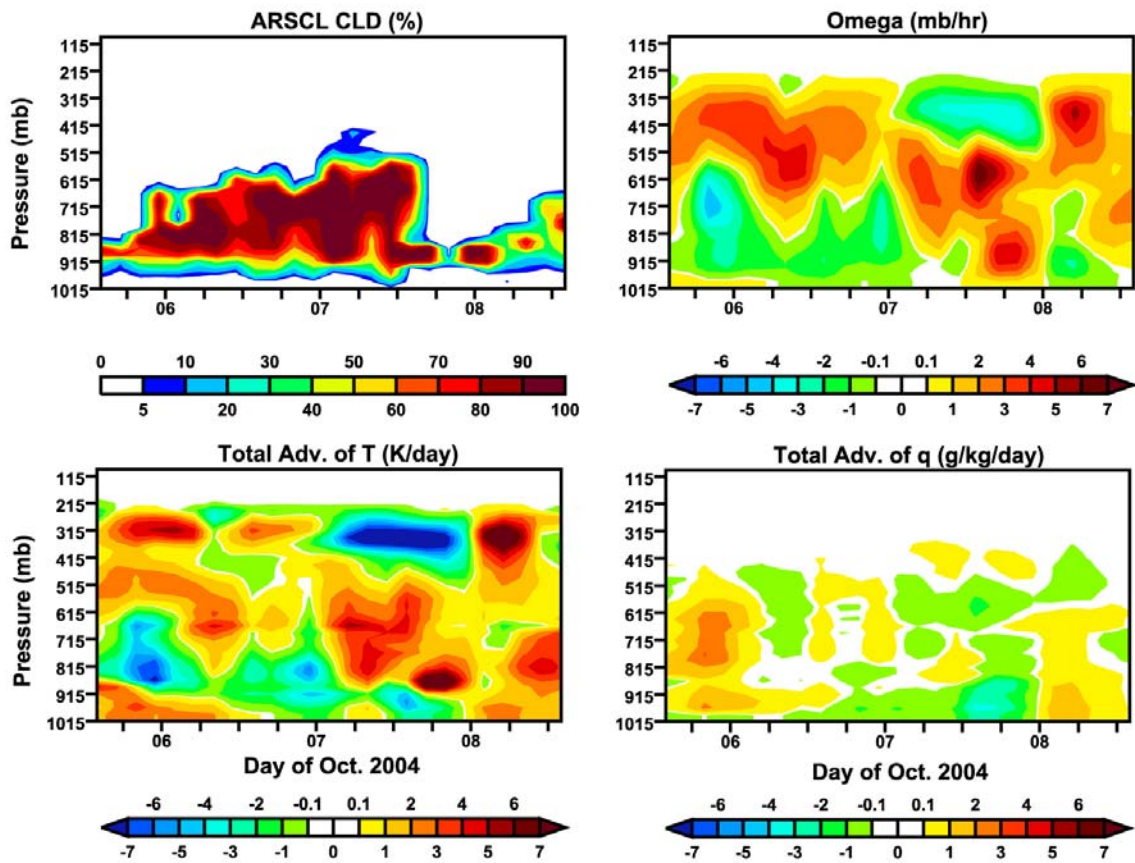


Figure 18. Period A conditions for ARSCL cloud from Barrow, and the vertical pressure velocity omega, and the total advective tendencies of temperature and water vapor from the variational analysis which will be specified in the models.

Data files containing forcing data and evaluation data are located at the ARM IOP Archive <http://iop.archive.arm.gov/arm-iop/0special-data/> then choose cpm-

forcing/iop_at_nsa/200410. A link to this archive is provided from the M-PACE website <http://science.arm.gov/wg/cpm/scm/scmic5>.

The vertical profiles are given in the files named `layer_0410_V1.1_STD.dat` and `surface_0410_V1.1_STD.dat`, both in ASCII text. For your convenience, a netCDF format of these data is also provided. Vertical profiles of observed large-scale temperature (\bar{T}), mixing ratio (\bar{q}), and velocity components (u , v , and w); the observed surface temperature (\bar{T}_s) and the surface pressure (\bar{p}_s); profiles of the observed large-scale *total* advective tendencies of temperature and mixing ratio, $(\partial\bar{T}/\partial t)_{L.S.}$ and $(\partial\bar{q}/\partial t)_{L.S.}$, and *horizontal* and *vertical* advective tendencies of temperature and mixing are contained here. The Fortran 77 programs to read ASCII forcing profiles data are also provided. Their names are: 'read_layer.for' and 'read_surface.for'.

Aerosol specifications

Please use the same specifications as were given for Period B. We are recommending this because (a) there was no usable data for the aerosol size distribution from the Aerosonde flights in Period A, and (b) the ice-nuclei concentrations from the Citation CFDC during the Period A flights show mean values and scatter similar to those recorded on the Period B flights. The mean ice nuclei concentration from the Citation flights on October 5, 6, and 8th were 0.114L^{-1} .

3 Sensitivity studies

It is assumed that the control simulation of each model will be carried out in its normal configuration. Besides this base simulation two sensitivity studies are asked for.

The first study is an integration of the model with all ice microphysics removed. That is, all clouds will be liquid water clouds. This permits an assessment of the degree to which ice microphysics alters cloud structure.

The second sensitivity study is one in which the vertical resolution is strongly increased. (A change in time step may also be needed to accomplish this increase in vertical resolution.) The vertical resolution will not be prescribed, but should be sufficient to resolve the vertical structures of the mixed phase clouds (i.e. the thin layers of liquid water cloud in Period A or the vertical increase with height of liquid water in the single layer stratocumulus of Period B). This resolution should be no coarser than 100 m.

4 Results to Submit

The results to be submitted will consist of *large-scale* quantities unless otherwise noted. Large-scale is defined as both a space and time average, indicated by an overbar. For CRMs or LES models, the space average is over all of the columns simulated in the model. SCM quantities already represent a space average in the horizontal direction over the SCM domain. The time average is the average over a 3-hour period for Period A and the average over 30 minutes (or the model time step if not convenient) for Period B. These averages should be based on “observations” taken frequently enough to avoid aliasing due to cloud-scale and mesoscale variability. Some quantities, such as surface rainfall and surface snowfall, should be accumulated every time step.

The large-scale quantities to be submitted will consist of time series and profiles at 3-hourly intervals for Period A and 30 minute intervals for Period B. The time series will be largely based on quantities provided in more detail in the profiles, so the latter will be described first.

See the CPM M-PACE Web page for instructions on where and how to submit model results.

4.1. Description of Experimental Quantities

4.1.1 Vertical profile quantities

Submit the results for each quantity listed below as a separate ASCII file in the file format described in 4.2.1. For a quantity not available in your model, a “dummy” file that is empty must be submitted. It should bear a proper name (as required of all profile quantities, in Section 4.1.3), but being suffixed with “.not_submitted”. In the following list, “(F*.*)” specifies the fortran ASCII data format.

Note: Because this list was devised for an intercomparison of models for cases involving deep convection, some of the quantities in the list below are not appropriate for the M-PACE intercomparison. Those quantities which are not relevant for the intercomparison are not requested for submission and are indicated below by brackets surrounding the number of the quantity, for example “[15.]”.

0. Pressure, \bar{p} (mb) (F7.1). Omit this file, if pressure is constant over time for all levels.
1. Height, \bar{z} (km) (F7.3). Omit this file, if height is constant over time for all levels.
2. Temperature, \bar{T} (K) (F7.2)
3. Water vapor mixing ratio, \bar{q} (g/kg) (F7.3)
4. Relative humidity, \bar{R} (unitless) (F6.3): $R=q/q^*(T,p)$, where $q^*(T,p)$ is the saturation mixing ratio over water.

Note: Do your best to report the mass of each type of hydrometeor below consistent with the microphysics contained in your model. If the definitions below – which are chosen to correspond

with the observations taken by the Citation aircraft – do not correspond well with the microphysics in your model, please indicate in the description of your model how you have chosen to report the hydrometeors in your model.

Note: Quantities 5-9 are horizontal averages over all areas – including those in which the hydrometeor is absent. In SCMs, this corresponds to the grid-box mean mass-mixing ratio and in CRMs or LES models, this is the horizontal average over all grid-cells including those in which the hydrometeor is absent.

5. Cloud water (suspended liquid water) mixing ratio, \bar{q}_c (g/kg) (F7.4): for bin-resolved microphysical models this will be the mass of liquid water droplets whose diameter is less than or equal to 50 micrometers.

6. Cloud ice (slow-falling, small ice) mixing ratio, \bar{q}_i (g/kg) (F7.4): for bin-resolved microphysical models, this will be the mass of ice crystals whose maximum dimension is less than or equal to 100 micrometers.

7. Rain (falling liquid water) mixing ratio, \bar{q}_r (g/kg) (F7.4): for bin-resolved microphysical models this will be the mass of liquid water droplets whose diameter is greater than 50 micrometers.

8. Snow (fast-falling low-density ice) mixing ratio, \bar{q}_s (g/kg) (F7.4): for bin-resolved microphysical models, this will be the mass of non-rimed ice crystals whose maximum dimension is greater than 100 micrometers.

9. Graupel (fast-falling high-density ice) mixing ratio, \bar{q}_g (g/kg) (F7.4): for bin-resolved microphysical models, this will be the mass of rimed ice crystals whose maximum dimension is greater than 100 micrometers.

10. Cloud fraction, $\bar{\sigma}$ (unitless) (F6.3): At each grid point, $\bar{\sigma} = 1$ if $\bar{q}_c + \bar{q}_i > 0.01 q^*(\bar{T}, \bar{p})$; otherwise, $\bar{\sigma} = 0$.

11. Horizontal wind velocity in x-direction, \bar{u} (m/s) (F7.2)

12. Horizontal wind velocity in y-direction, \bar{v} (m/s) (F7.2)

13. Apparent heat source, Q_{1C} (K/day) (F7.2):

$$Q_{1C} \equiv Q_1 - Q_R = \left[\bar{\sigma} \bar{T} / \partial t - (\partial \bar{T} / \partial t)_{L.S.} \right] - Q_R$$

14. Apparent moisture sink, Q_2 (K/day) (F7.2):

$$Q_2 = - \frac{L}{c_p} \left[\bar{\sigma} \bar{q} / \partial t - (\partial \bar{q} / \partial t)_{L.S.} \right]$$

[15.] Convective Q_{1C} , Q_{1C}^c (K/day) (F7.2): Contribution to Q_{1C} from the “convective” columns.

[16.] Stratiform Q_{1C} , Q_{1C}^s (K/day) (F7.2): Contribution to Q_{1C} from the “stratiform” columns.

[17.] Convective Q_2 , Q_2^c (K/day) (F7.2): Contribution to Q_2 from the “convective” columns.

[18.] Stratiform Q_2 , Q_2^s (K/day) (F7.2): Contribution to Q_2 from the “stratiform” columns.

19. Radiative heating rate, Q_R (K/day) (F7.2)

20. Solar (short-wave) radiative heating rate, Q_R^{SW} (K/day) (F7.2)

21. Infrared (long-wave) radiative heating rate, Q_R^{LW} (K/day) (F7.2)

[22.] Clear radiative heating rate, Q_R^{clr} (K/day) (F7.2): The average radiative heating rate in the “clear” columns.

[23.] Cloudy radiative heating rate, Q_R^{cld} (K/day) (F7.2): The average radiative heating rate in the “cloudy” columns.

[24.] Cloud mass flux, M_c (mb/s) (F8.5): $M_c = M_u - M_d$

[25.] Updraft cloud mass flux, M_u (mb/s) (F7.5):

$$M_u = \frac{\sum_j \sigma \omega^+}{\sum_j},$$

where j is the grid point column index, σ is the cloud fraction (defined previously), $\omega^+ = \omega$ if $\omega < 0$, otherwise, $\omega^+ = 0$.

[26.] Downdraft cloud mass flux, (mb/s) (F7.5): $M_d = M_{ds} + M_{du}$,

where M_{ds} and M_{du} are the saturated and unsaturated downdraft cloud mass fluxes:

$$M_{ds} = \frac{\sum_j \sigma \omega^-}{\sum_j}$$

and

$$M_{du} = \frac{\sum_j \sigma_p \omega^-}{\sum_j}.$$

Here, $\omega^- = |\omega|$ if $\omega > 0$, otherwise, $\omega^- = 0$. Also, $\sigma_p = 1$ if $\sigma = 0$ and $q_r + q_s + q_g > P$, with $P = 0.1$ g/kg; otherwise, $\sigma_p = 0$.

[27.] Fractional area of updraft cores, $\overline{\sigma_u}$ (unitless) (F6.3): A “core” exists if $|\omega| > W$, with $W = 0.1$ mb/s. Thus,

$$\overline{\sigma_u} = \frac{\sum_j \sigma_u}{\sum_j}$$

where $\sigma_u = 1$ if $\omega < -W$; otherwise, $\sigma_u = 0$.

[28.] Fractional area of downdraft cores, $\overline{\sigma_d}$ (unitless) (F6.3):

$$\overline{\sigma_d} = \frac{\sum_j \sigma_d}{\sum_j},$$

where $\sigma_d = 1$ if $\omega > W$; otherwise, $\sigma_d = 0$.

[29.] Average core updraft speed, ω_u (mb/s) (F7.3):

$$\omega_u = \frac{\sum_j \sigma_u \omega}{\sum_j \sigma_u}.$$

[30.] Average core downdraft speed, ω_d (mb/s) (F7.3):

$$\omega_d = \frac{\sum_j \sigma_d \omega}{\sum_j \sigma_d}.$$

31. Hydrometeor fraction, $\overline{\sigma_h}$ (unitless) (F6.3): At each grid point, $\sigma_h = 1$ if $\sigma = 1$ or $q_r + q_s + q_g > E = 10^{-3}$ g/kg; otherwise, $\sigma_h = 0$.

Note that quantities 32 to 37 are averages for the volumes in which the hydrometeors exist.

32. Liquid cloud droplet effective radius $r_{eff,l}$ (microns) (F7.2)

33. Ice crystal effective size $r_{eff,i}$ (microns) (F7.2)

34. Cloud droplet number (cm^{-3}) (F7.1)

35. Cloud ice number concentration (per liter) (F7.1)

36. Snow number concentration (per liter) (F7.1)

37. Graupel number concentration (per liter) (F7.1)

4.1.2 Time-series quantities

Submit the results for each of the three groups of quantities listed below, each group in a separate ASCII file, as described in Section 4.2.2. For any quantity that is not available in your model, a required “fill” value must appear in its position, as a constant over time (4.2.2, Note C). If all quantities in a group are unavailable, a dummy file that’s empty should be created, and given with the file name suffix “.not_simulated”.

In the following list, “(F*.)” and “(E*.)” specifies the fortran ASCII data format.

Group 1:

1. Time of mid-point of averaging interval, \bar{t} (h) (F6.1)
2. Surface skin temperature, SST (K) (F7.2)
3. Near-surface dry static energy, $\overline{s_0}$ (kJ/kg) (F7.2): $s = c_p T + gz$. “Near-surface” is the first model level above the surface.
4. Near-surface water vapor mixing ratio, $\overline{q_0}$ (g/kg) (F6.2)
5. Near-surface moist static energy, $\overline{h_0}$ (kJ/kg) (F7.2): $h = s + Lq$.
6. Near-surface horizontal wind velocity in x-direction, $\overline{u_0}$ (m/s) (F7.2)
7. Near-surface horizontal wind velocity in y-direction, $\overline{v_0}$ (m/s) (F7.2)
8. Surface turbulent flux of sensible heat, $\overline{(F_s)_0}$ (W/m^2) (F6.1): $F_s \equiv \rho c_p \left(\frac{p_0}{\bar{p}} \right)^{R/c_p} \langle \omega T' \rangle$.
9. Surface turbulent flux of latent heat, $\overline{L(F_q)_0}$ (W/m^2) (F6.1): $F_q \equiv \rho \langle \omega' q' \rangle$.
10. Surface turbulent flux of horizontal momentum component in x-direction, $\overline{(F_u)_0}$ (nt/m^2) (F8.4): $F_u \equiv \rho \langle u' \omega' \rangle$.
11. Surface turbulent flux of horizontal momentum component in y-direction, $\overline{(F_v)_0}$ (nt/m^2) (F8.4): $F_v \equiv \rho \langle v' \omega' \rangle$.

[12.] Boundary layer depth, \overline{Z}_i (m) (F6.0). Note: we may choose to compute a boundary layer depth by applying a single algorithm to the temperature and water vapor profiles we receive.

Group 2:

1. Time of mid-point of averaging interval, \bar{t} (h) (F6.1)
2. Surface downwelling solar radiative flux, $\left(\overline{F_{SW}^-}\right)_0$ (W / m^2) (F7.1)
3. Surface upwelling solar radiative flux, $\left(\overline{F_{SW}^+}\right)_0$ (W / m^2) (F7.1)
4. Surface downwelling infrared radiative flux, $\left(\overline{F_{LW}^-}\right)_0$ (W / m^2) (F6.1)
5. Surface upwelling infrared radiative flux, $\left(\overline{F_{LW}^+}\right)_0$ (W / m^2) (F6.1)

Note: Because LES models do not simulate the full vertical extent of the atmosphere, they will not submit quantities 6-8.

6. TOA (top of atmosphere) downwelling solar radiative flux, $\left(\overline{F_{SW}^-}\right)_T$ (W / m^2) (F7.1)
7. TOA upwelling solar radiative flux, $\left(\overline{F_{SW}^+}\right)_T$ (W / m^2) (F6.1)
8. TOA upwelling infrared radiative flux (OLR), $\left(\overline{F_{LW}^+}\right)_T$ (W / m^2) (F6.1)
9. Cloud amount, $\overline{A_{cld}}$ (unitless) (F6.3): Fraction of columns which are “cloudy” for CRMs. (“Cloudy” is defined as in profile quantity #10.) For SCMs, this quantity is the vertically projected cloud fraction (sometimes called “total cloud fraction”) and depends on cloud layer overlap assumptions.
- [10.] Cold cloud top area, $\overline{A_{cld}^{cold}}$ (unitless) (F6.3): Fraction of columns for which the “cloud top temperature” is less than 245 K.
11. Precipitable water, PW (kg / m^2) (F6.2): $PW = \int_0^{z_T} \rho q \, dz$, where z_T is the model top height.
(Note: LES models need to report their model top.)
12. Cloud liquid water path, LWP (kg / m^2) (E10.3): $LWP = \int_0^{z_T} \rho q_c \, dz$.
13. Cloud ice path, IWP (kg / m^2) (E10.3): $IWP = \int_0^{z_T} \rho q_i \, dz$.

Group 3:

1. Time of mid-point of averaging interval, \bar{t} (h) (F6.1)
2. Vertically integrated rain, RP (kg / m^2) (E10.3): $RP = \int_0^{z_T} \rho q_r \, dz$.

3. Vertically integrated snow, SP (kg / m^2) (E10.3): $\text{SP} = \int_0^{z_T} \rho q_s dz$.
4. Vertically integrated graupel, GP (kg / m^2) (E10.3): $\text{GP} = \int_0^{z_T} \rho q_g dz$.
5. Surface rain rate, \bar{P}_{rain} (mm/day) (F7.2): Note: Please provide the accumulated rainfall over the reported time interval.
- [6.] Convective surface rainfall rate, \bar{P}_c (mm/day) (F7.2): The contribution to \bar{P} from the “convective” columns.
- [7.] Stratiform surface rainfall rate, \bar{P}_s (mm/day) (F7.2): The contribution to \bar{P} from the “stratiform” columns.
- [8.] Rain fractional area, \bar{A}_r (unitless) (F6.3): Fraction of columns which are “rainy.”
- [9.] Convective fractional area, \bar{A}_c (unitless) (F6.3): Fraction of columns which are “convective.”
- [10.] Stratiform fractional area, \bar{A}_s (unitless) (F6.3): Fraction of columns which are “stratiform.”
11. Surface “snow” rate, \bar{P}_{frozen} (mm/day) (F7.2): Note: Provide the accumulated surface frozen hydrometeors (ice, snow, and graupel) over the reported time interval.

4.1.3 How these quantities are to be directed to files, and how the files named

Each vertical profile quantity is to be written out to a separate data file. For time-series quantities, each of their three groups, as defined above, should be written to a separate file. These files should be in ASCII text formats, as defined in Section 4.2. This has been the easiest way for the vast majority of participants, in which to submit data. However, we will convert submitted data files into the ARM standard format, which is netCDF based, for each participant as soon as the ASCII data files submitted are checked out for readability.

Examples of file names for data simulated:

Example of a file containing a profile quantity

- *b1.p4.CCM3_SUNY* -- where ‘b’ is a low-case letter indicating the sub-period simulated (period A or period B);
- ‘1’ is a digit (a dummy constant for now) which is required indicates experimental versions. For this intercomparison, 1 = base case, 2 = no ice microphysics run, 3 = increased vertical resolution.
- ‘p4’ indicates a [vertical] profile file containing the quantity number 4 in Section 4.1.1;

- “CCM3_SUNY” is the acronym of your model name, one used (or to be used) in publication. It should not exceed 13 characters and must *not* include any character that has a reserved meaning on the Unix command line (e.g., /, &, \, and any bracketing char.) Please use the *underscore in lieu of the slash* if the latter is part of your acronym, for the purpose of naming your files.

Example of a file containing a group of time-series quantities

b1.t2.CCM3_SUNY -- where

- ‘b’, ‘t’, and ‘CCM3_SUNY’ are the same as above;
- ‘t’ indicates a time-series file;
- ‘2’ indicates this file contains the n-th group of time-series variables (where n = 2 in this example), per Section 4.1.2.

Note: *Dummy (empty) files are required for data not simulated.*

Examples – of file names for data not simulated:

b1.p31.CCM3_SUNY.not_submitted

where ‘p31’ indicates the vertical profile quantity numbered 31 per Section 4.1.1.

b1.t3.CCM3_SUNY.not_submitted

where ‘t3’ indicate none of the time-series quantities in group 3 is available.
(If some but not all are missing, consult Note C in Section 4.2.2.)

4.2. Formats for Data Files to be Submitted

4.2.1 Format for a .p file containing a profile variable

Submit the results for each quantity listed above as a separate ASCII file in the file format described in this subsection. Include the time (since initiation time for the sub-period in the forcing data), to the midpoint of the averaging interval of time (hours, F6.1); and also, either (a) the pressure p (mb, F7.3) or (b) the height z (km, F7.3), whichever is independent variable that is constant over time for every vertical level. If omega levels are used, we expect that you can easily supply mean pressures for the sub-period at these levels, as part of the coordinate variable.

Important: If for your model either p or z changes over time, we need you to supply the .p0 (pressure data 2-D array) or .p1 (height data 2-D array) respectively – each in a separate file, in the same manner as for all experimental quantities. If omega levels are used, you must supply both .p0 and .p1 files.

New: Immediately upon generating your .p files, please check the third line of each file to make sure that none of them has either the “maxes” or “mins” lines corrupted with bad characters, indicating format over- or underflow errors.

In the following illustration:

$nlev$ is the number of pressure levels reported;

nt is the number of time steps reported;

f_{max} , f_{min} are the minimum and the maximum value of the data - see Note A

$p(ip)$ pressure value at ip -th level (from ground toward TOA)

$t(it)$ is time value at it -th sample reported

$f(t(it), p(ip))$ is the data value associated with the above.

The first line of each file is a comment line, that begins with the identifier #, followed by the filename, and then optionally, any further distinguishing characteristics.

The file structure is line-by-line and blank-delimited, as follows:

```
#Name_of_file model_description(/variant) fieldname(units) Comment (if any)
nlev nt
f_max f_min
p(1_nearest-to-ground) p(2) p(3) ... p(10)
p(11) ... p(nlev-1) p(nlev)
t(1) t(2) t(3) ... t(10)
t(11) t(12) t(13) ... t(20)
...
... t(nt-1) t(nt)
f(t(1),p(1)) f(t(2),p(1)) f(t(3),p(1)) ... f(t(10),p(1))
f(t(11),p(1)) f(t(12),p(1)) f(t(13),p(1)) ... f(t(20),p(1))
f(t(21),p(1)) f(t(22),p(1)) f(t(23),p(1)) ... f(t(30),p(1))
...
... f(t(nt-1),p(1)) f(t(nt),p(1))
f(t(1),p(2)) f(t(2),p(2)) f(t(3),p(2)) ... f(t(10),p(2))
f(t(11),p(2)) f(t(12),p(2)) f(t(13),p(2)) ... f(t(20),p(2))
f(t(21),p(2)) f(t(22),p(2)) f(t(23),p(2)) ... f(t(30),p(2))
...
... f(t(nt-1),p(2)) f(t(nt),p(2))
.....
.....
f(t(1),p(nlev)) f(t(2),p(nlev)) f(t(3),p(nlev)) ... f(t(10),p(nlev))
f(t(11),p(nlev)) f(t(12),p(nlev)) f(t(13),p(nlev)) ... f(t(20),p(nlev))
f(t(21),p(nlev)) f(t(22),p(nlev)) f(t(23),p(nlev)) ... f(t(30),p(nlev))
... f(t(nt-1),p(nlev)) f(t(nt),p(nlev))
```


Note A --

The *f_max,f_min* line contains the maximum value and minimum value, written in *the same elemental data format* as you use in writing all data values for the variable.

4.2.2 Format for time series quantities for a .t file, containing time-series variables

Submit the results for each of the three groups of quantities listed above as a separate ASCII file.

The first line of each file is a comment line, that begins with the identifier #, followed by the filename, and then optionally, any further distinguishing characteristics.

New: After the comment line, come three more header lines: a line containing *nt* (number of time steps reported); the so-called “maxes” line, which contains the maximum values of the variables reported, preceded by the dummy time value +999.9; and the so-called “mins” line containing the minimum values preceded by the dummy time value -999.9. The latter two lines must have the same format as used for the time-series data lines which follow.

New: Immediately upon generating your .t files, please check the top three lines of all files to make sure that none of them has either the “maxes” or “mins” line corrupted with bad characters, indicating format over- or underflow errors.

Following the comment line and the line containing *nt*, the structure of the file can be, optionally, either one of fixed formats as illustrated below (and specified in *Note B-1*) or free formatted with delimiting blanks and fields of comparable precision, of your own choice (*Note B-2*). See *Note C* for a general note on how to handle missing – not simulated variables.

In the following illustration:

nt is the number of time steps reported;

Gnf1 stands for Group_n field_1;

Gnf2 stands for Group_n field_2; etc.

max(Gnf1) stands for the maximum value for *Gnf1* (see *Note A-1*)

#Name_of_file Model[/variant]_description Comment (if any)

nt

+999.9*max(Gnf1)max(Gnf2)max(Gnf3)max(Gnf4)...*

-999.9*min(Gnf1)min(Gnf2)min(Gnf3)min(Gnf4)...*

time(1)Gnf1(time(1))Gnf2(time(1))Gnf3(time(1))Gnf4(time(1))...

time(2)Gnf1(time(2))Gnf2(time(2))Gnf3(time(2))Gnf4(time(2))...

...

...

time(nt)Gnf1(time(nt))Gnf2(time(nt))Gnf3(time(nt))Gnf4(time(nt))...

Note A-1 --

The maxes and the mins line should have the same format for the data lines that follow them, as explained next.

Note B-1--

Suggested format specifications for each time-series group are as follows, in Fortran notation. It is not necessary to add delimiting blanks between the elemental formats (individual variable values). (It won't hurt though, since the blanks will just make your data conformant to the free field format, as in *Note B-2*.)

The suggested formats are as follows:

- group 1 (F6.1,2F7.2,F6.2,3F7.2,2F6.1, 2F8.4,F6.0);
- group 2 (F6.1,2F7.1,2F6.1,F7.1,2F6.1,2F6.3,F6.2,2E10.3);
- group 3 (F6.1,3E10.3,3F7.2,3F6.3,F7.2).

Note B-2 –

Also acceptable is blank-delimited field formats of your own choosing – one line per time step - consistently from line to line. The E*.* (exponential) format is preferred (over fixed point) avoid any problem with precision. Whatever you do, do the same for the “maxes” and the “mins” line.

Note C --

If you don't plan on submitting a certain field, please write in its format space a negative number with all decimal positions being '8' -- except the exponent positions, which can be just '+00' or '+01'. If all fields in a certain group are unavailable, see Section 3.1.3, regarding the dummy/empty file required.

5 Model Descriptions

In order to compare results from different models, workshop participants are asked to complete the following description relevant for simulations performed for the intercomparison. This description will help to build up the workshop report at the final stage. The following items apply to both SCMs and CRMs/LES. Respond only to those that apply to your SCM. Note that the main science theme of MPACE intercomparison is to understand what determines the cloud amount, phase, morphology, and time evolution in observations and in models. Please provide more detailed information on the cloud parameterizations. In particular, we ask for detailed information on the parameterizations of cloud microphysics, especially those that would affect the simulation of mixed phase clouds.

Scientist:

- Name
- Affiliation
- Address
- Email address
- Fax number

Model Name and History:

- Long name [model/variant]
- Acronym (to be used in graphics & data files naming)
- Short/conversational name (other than acronym, if any)
- Generic predecessor or relative (name/variant, and acronym, whether or not it also takes part in this study)

On attributes listed below, please be as complete as would be required to satisfy the editor of a journal article.

For each additional model you have participating in this study, you need to fill out a separate page. With proper reference, omission of redundant attribute information is allowed (if you write “AsGP” or “AsGR” (As its Generic Predecessor or Relative), and have cited the prior model, where asked (as above).

Model Type: (1D, 2D, 3D)

Numerical Domain:

- Domain size in x-direction:
- Domain size in y-direction:
- Domain size in z-direction:
- Number of grid points in x-direction:
- Number of grid points in y-direction:
- Number of grid points in z-direction:

- Grid size in x-direction:
- Grid size in y-direction:
- Grid size in z-direction (if stretched please specify):
- Time step

Numerical Technique:

- Numerical method (finite-difference, spectral, etc.):
- Advection scheme and its order of accuracy:
- Time scheme and its order of accuracy:
- Dynamical equations (elastic, anelastic, etc.):
- Numerical diffusion (type, order, magnitude of coefficient)
- Lateral boundary conditions:
- Upper boundary condition (Sponge layer, specification, ...):
- Translation velocity of the reference frame
- Other information

Physical Parameterizations:

- Surface flux parameterization for heat, moisture, momentum:
- Longwave radiation parameterization:
- Shortwave radiation parameterization:
- How were radiative fluxes above the computational domain handled?
- Microphysical (2D/3D models) or cloud/convective (1D model) parameterization: type, number of hydrometeor classes, ...
- Turbulence closure scheme (turbulence closure type, variables predicted and diagnosed by - - the turbulence closure, closure for turbulent length scale, ...)
- Other information

Documentation:

Please provide references that more fully describe your model.

- Documentation (present model), if available.
- Documentation (predecessor or relative) – optional if the preceding is available.

6 Time Table

6.1 Soliciting & Accepting Preliminary Results

By September 1, 2006

- Declare interest in joining the preliminary study, by sending E-mail to Stephen.Klein@arm.gov
- Watch for updates on this document, and its new requirements (if any). <http://science.arm.gov/wg/cpm/scm/scmic5>
- Conduct simulation runs – per updated requirements; and submit results, and see them through verification and acceptance.

6.2 Processing & Comparing Preliminary Results

September - October 2006

- View results of evaluation and intercomparison of models.
- Download netCDF or ASCII data, for your own use.

6.3 Results Discussion

October 30-31, 2006

- CPM Fall Meeting in San Francisco, California